Sixth International Conference on Durability of Concrete Structures **Paper Number TIM14**
18 - 20 July 2018
University of Leeds, Leeds, West Yorkshire, LS2 9JT, United Kingdom

Similarity Analysis of Rebar Corrosion under Different Electrochemical Accelerated Method

C. Fu, J. Chen and X. Jin
College of Civil Engineering and Architecture, Zhejiang University of Technology, Hangzhou, China

H. Ye
Department of Civil Engineering, The University of Hong Kong, Pokfulam, Hong Kong, China

Jun Zhu
College of Mechanical Engineering, Zhejiang University of Technology, Hangzhou, China

ABSTRACT

The concrete cover cracking caused by non-uniform corrosion of reinforcing bar is one of the most important reason for structure service performance degradation. The most widely used electrochemical accelerated corrosion methods include external and internal electrode methods. The reinforcement are used as anode in both methods. The different between two methods is the position of auxiliary. In external electrode method, the auxiliary is set outside the specimen, including three methods, i.e. samples whole/part submerged in saline, samples wrapped by sponge and steel mesh. The electrochemical mechanism of these four accelerated method were analyzed by using the FE software COMSOL. According to the corrosion products distribution characteristic along the rebar circumference, the similarity of electrochemical accelerated and natural corrosion was presented. The results indicated that, rebar corrosion with external electrode method can be regarded as uniform corrosion; the internal electrode method could result in a non-uniform corrosion after optimizing, and the orientation and distance of rebar/electrode are two major influence parameters for accelerated non-uniform corrosion. In addition, based on the corrosion electrochemical principles, a modified internal electrode method was given. The stainless wire was put into the cylinder samples parallel to the rebar as a cathode. In present study, the rapid non-uniform corrosion method can play a positive role in studying the cover cracking process of reinforced concrete.

Key words: rebar; non-uniform corrosion; similarity; accelerated corrosion; natural corrosion

1.0 INTRODUCTION

Corrosion of steel reinforcement has been one of the most common problem globally which will result in the formation of longitudinal cracks, peeling-off of concrete cover, degradation of steel-concrete bonding, as well as reduction of structural bearing capacity an ductility (Ye *et al*. 2013). Because of the significance of this issue, a tremendous amount of work has been done over decades, including, the crack shapes and rust distribution patterns around the corroded rebar (Cao *et al*. 2014), the prediction of concrete cover cracking initiation time (Zhang *et al*. 2015), the relationship between corrosion-induced crack widths and rust formation (Oh *et al*. 2009), among others.

Three laboratory techniques are widely used for studying the corrosion characteristics of rebar in RC structures in previous studies, namely, natural exposure (Fu *et al*. 2017), accelerated corrosion using artificial climate environments (Yuan *et al*. 2007), accelerated corrosion using galvanic method (El Maaddawy *et al*. 2003). Previous studies concluded that natural corrosion and accelerated corrosion using artificial climate environments show similar corrosion characteristics (Yuan *et al*. 2007). Nevertheless, due to short acceleration duration and high repeatability, galvanic methods are still adopted widely in the world. The most widely used electrochemical accelerated corrosion methods include external and internal electrode methods. The reinforcement are used as anode in both methods. The different between two methods is the position of auxiliary. In external electrode method, the auxiliary is set outside the specimen, including three methods, i.e. samples whole/part submerged in saline and samples wrapped by sponge and steel mesh. This study attempts to analyze the electrochemical mechanism of these four accelerated method and to present the similarity of electrochemical accelerated and natural corrosion.

2.0 BACKGROUND OF ACCELERATED ELECTROCHEMIACL CORROSION

The main ingredient of reinforcement is iron, which also contains carbon, manganese, silicon, phosphorus, sulfur and some other impurities. These elements exist in different forms such as cementite, austenite and martensite. Due to the potentials are different between different components of reinforcement, a lot of micro batteries will be formed in the surface of reinforcement when there are water film and dissolved oxygen. Because concrete is a kind of heterogeneous material, many of these micro batteries may occur at the early stage of the corrosion in small range. In most cases, macro uniform corrosion of the steel bar is the result of these micro batteries. In the later period, with the rust growing and the chloride accumulating, the corrosion of the macro battery between steel and rust will form. This is a typical spontaneous REDOX reaction, strong oxidizing material and strong reductive material react to produce weak oxidizing substances and weak reductive substances.

In contrast to the above, the galvanic accelerated corrosion test is an artificial macro battery reaction. It is to accelerate electrochemical reaction to accelerate the corrosion of reinforcement by applying an external current to reinforcement (Fig.1).

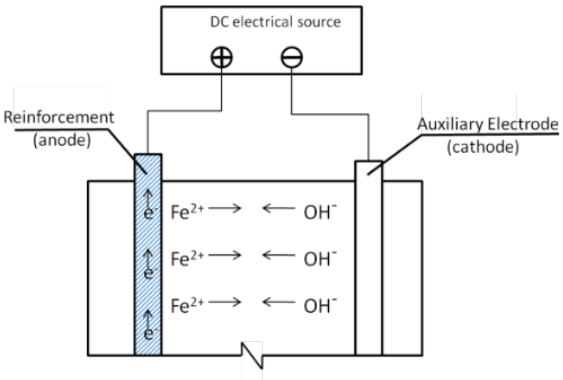

Fig.1. Schematic diagram of accelerated corrosion methods

The reinforcement is connected to the anode and the auxiliary electrode is connected to the cathode. Under the action of the current, two electrochemical half-cell reactions will take place at the electrode surface. At reinforcement, the anode half-cell action liberates electrons, which will let the iron oxidize to Fe^{2+}.The auxiliary electrode gets electrons. Then the water is deoxidized to OH^-.To end the circuit, an ionic exchange current through the electrolyte(concrete pore solution).Typically, the half-cell reaction for accelerated corrosion of reinforcement can be described as(Revie, 2008):

Anode:

$$Fe - 2e^- \rightarrow Fe^{2+} \quad (1)$$

Cathode:

$$2H_2O + 2e^- \rightarrow H^2\uparrow + 2OH^- \quad (2)$$

Once corrosion is started, the potentials of the half-cell reactions are shifted from equilibrium potential, which is known as polarization. The degree of polarization is typically measured by the overpotential which controls the kinetics of the electrochemical half-cell reactions. The overpotential can be defined as $\eta_{a/c} = E_{a/c} - E^0_{a/c}$, in which $E_{a/c}$ is the corrosion potential and $E^0_{a/c}$ is the equilibrium potential(the subscript a represent anode and c represent cathode).

Concentration polarization, activation polarization and potential drop (i.e., IR drop) are three basic causes of polarization. The concentration polarization can be ignored because of anode and cathode reactions occur so rapidly during galvanic accelerated corrosion. For activation polarization, according to Butler-Volmer equation, the relation between current density and the overpotential can be described as follow (Mann *et al*. 2006):

$$i_a = i_a^0 \left[\exp\left(\frac{\alpha nF}{RT} \eta_a \right) - \exp\left(-\frac{\beta nF}{RT} \eta_a \right) \right] \quad (3)$$

$$i_c = i_c^0 \left[\exp\left(\frac{\alpha nF}{RT} \eta_c \right) - \exp\left(-\frac{\beta nF}{RT} \eta_c \right) \right] \quad (4)$$

in which, i_a and i_c are the corrosion current density of anode and cathode, respectively; i_a^0 and i_c^0 are the exchange current density of the anode and cathode, respectively; α and β are charge transfer coefficient; η_a and η_c are the overpotential of anode and cathode, respectively; F is the Faraday's constant; T is the absolute temperature; R is the universal gas constant.

When the external voltage application, according to Ohm's law, the following equation must be satisfied:

$$E_{cell} = E_a + E_c + IR_s \quad (5)$$

in which, E_{cell} is the potential of the applied external source; IR_s is the ohmic drop where I is the current of the electrochemical system and R_s is the electrolytic resistance of concrete between anode and cathode, which can be define as $R = \rho\frac{L}{S}$; ρ is the resistivity between anode and cathode; L is the length of the charge path between anode and cathode; S is the area of the charge path which is related to ratio between anode and cathode surface area.

The current intensity value can be obtained by the surface integration of the current densities, and further related to the overpotential by Butler-Volmer equations (Eqs.(3)and(4)).After solving a series of

nonlinear mathematical equations composed of Eqs. (3)-(5),the corrosion current density distribution can be obtained.

From Eqs. (3)-(5), we can infer that distance between electrodes and ratio between electrodes are parameters of corrosion current density distribution. Therefore, the corrosion current density distributions of four kinds of galvanic accelerated corrosion methods are different.

3.0 PRELIMINARY EXPERIMENTATION

3.1 Materials

The concrete was designed to have a compressive strength of about 40MPa.The specimen were prepared by mixing OPC, water, sand, and stone in a ratio of 1:0.53:2.0:3.0 (kg/m^3). The OPC was P•I 52.5 Portland cement produced by China Huaxin cement factory, and the water is tap water. The concrete cubes with the dimensions of 100 mm × 100 mm × 100 mm was found have a 28-day average compressive strength of 45.6 MPa.

3.2 Specimen preparation

The configuration of test specimen is shown in Figs. 2 and 3.The specimen A is for external electrode methods, i.e. samples whole/part submerged in saline and samples wrapped by sponge and steel mesh. The specimen B is for internal electrode methods. It can be seen that for each specimen, it was basically a cube with the dimensions of 100 mm × 100 mm × 100 mm. For both specimens, the steel bar with the diameter of 10 mm was embedded in the side of the cube. The cover thickness was 20 mm. For the specimen B, a stainless steel bar with a diameter of 10mm was embedded in the other side of the concrete cube, which was symmetrical with reinforcement. Then in order to prevent the effect of exposed bars, the end of bars were coated with epoxy resin. After casting, all specimens were cured in an environmental chamber with 65±5 % relative humidity and 20±2 ^{0}C for 28 days.

3.3 Accelerated corrosion method

After curing, the corrosion of steel embedded in the concrete was accelerated by galvanic method as elaborated later. In order to galvanization, the specimens were first immersed into the 5 % sodium chloride solution before the experiment. It was believe that the steel corrosion has initiated with destroyed passive film. The impressed current density was controlled to be around 15 A/m^2, which followed the previous studies (Yuan *et al*. 2006). The galvanic methods are as follows:

(a) External electrode method, in which the whole sample was submerged in saline (Fig. 4).
(b) External electrode method, in which samples part submerged in saline (Fig. 5).
(c) External electrode method, in which samples wrapped by sponge and stainless mesh (Fig.6).
(d) Internal electrode methods (Fig.7).

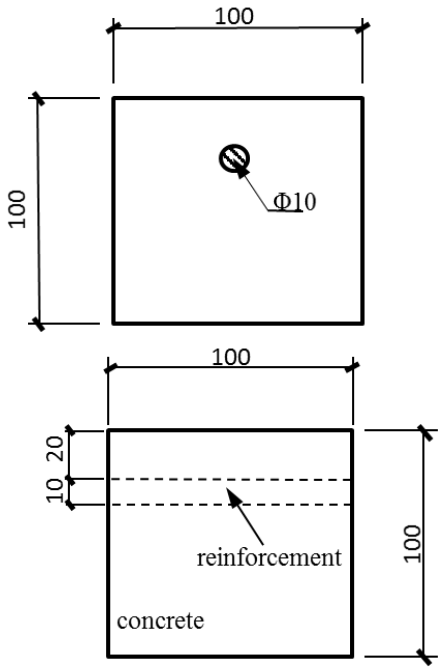

Fig. 2. Configuration of the designed specimen A (Unit: millimeter)

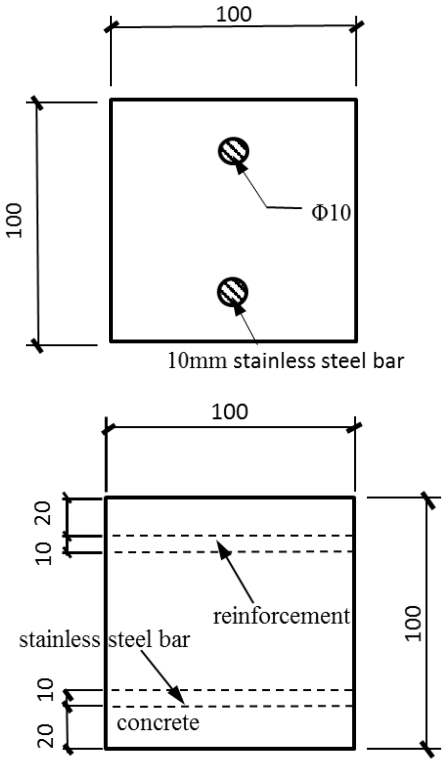

Fig. 3. Configuration of the designed specimen B (Unit: millimeter)

(a) External electrode method, in which the whole sample was submerged in saline (Fig. 4)
During the corrosion acceleration, the steel was connected to the anode while the auxiliary electrode (stainless bar) was connected to the cathode. The specimens were completely immersed in 6% NaCl solution in the whole process of acceleration.

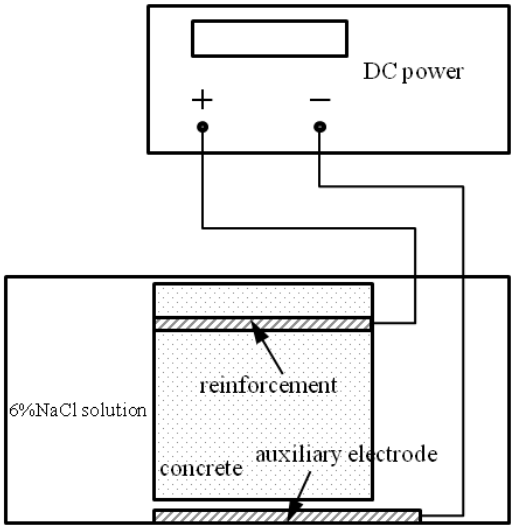

Fig. 4. Accelerated corrosion with external electrode method, in which samples whole submerged in saline

(b) External electrode method, in which samples part submerged in saline (Fig. 5)
The method is roughly the same as the previous method. However, the specimen was partially immersed in 6% NaCl solution in this test.

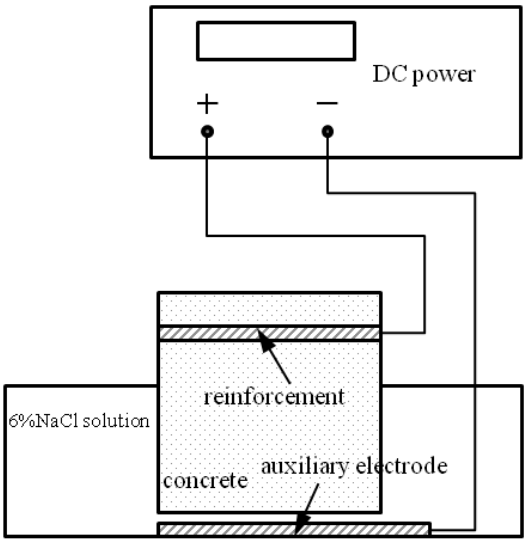

Fig. 5. Accelerated corrosion with external electrode method, in which samples part submerged in saline

(c) External electrode method, in which samples wrapped by sponge and stainless mesh (Fig.6)
As shown in the figure, the surface of the specimen was coated with a layer of sponge material saturated with 6% NaCl solution, and a stainless wire mesh wrapped on the outside. During the corrosion acceleration, the steel was connected to the anode while the stainless wire mesh was connected to the cathode.

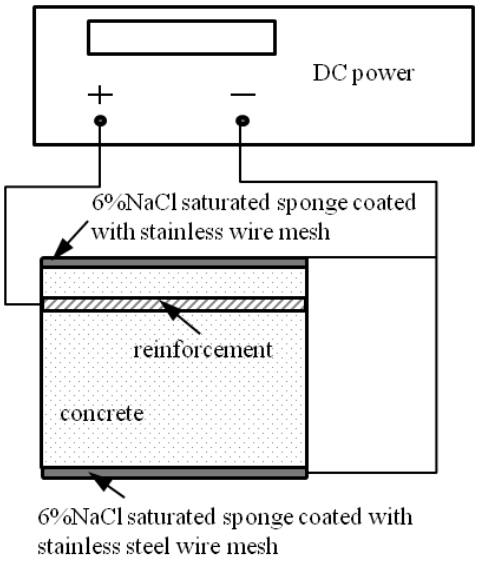

Fig.6. Accelerated corrosion with external electrode method, in which samples wrapped by sponge and stainless mesh.

(d) Internal electrode methods (Fig.7)
In this method, the auxiliary electrode (stainless steel bar) is precast in the concrete specimen. When test was conducted, the steel was connected to the anode and the stainless steel bar was connected to the cathode.

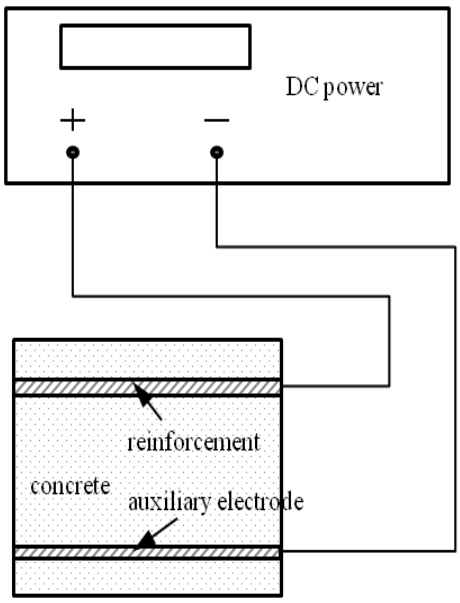

Fig.7. Accelerated corrosion with internal electrode method

In order to keep the wire properly connected and the current density maintained in 15 A/m^2, periodic

inspection was performed on every 12h during the acceleration. For method (1) and (2), the NaCl solution was stirred to ensure that the solution concentration and depth remains the same. At the same time, the corrosion products on the auxiliary electrode was cleaned in time to ensure that the corrosion rate is not affected by the accumulation of rust. For method (3) and (4), 6% NaCl solution was regularly sprayed to keep specimen wet. The acceleration was carried out until specimen cracked.

3.4 Observation of Specimens

The specimen was cut and observation to study the rust distribution around steel cross section under different galvanic methods. In order to eliminate the influence of the two ends (i.e. top and bottom) of specimens, the cutting position was set in the middle of specimens.CMS-200 optical microscope produced by Shanghai Changfang optical instrument Company was adopted. The adopted equipment can clear distinguish the steel, rust and concrete and provided the function of distance measuring. The measurement accuracy is 0.001 mm.

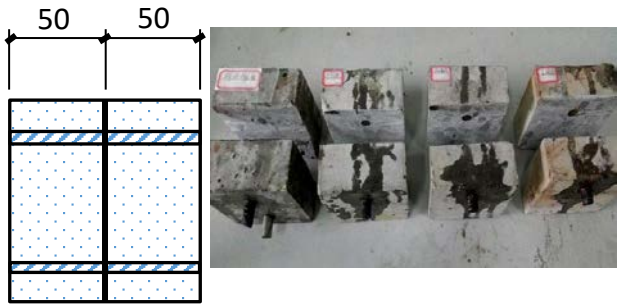

Fig. 8. Cutting position of specimens

3.5 Results and Discussion

Through analysis the data measured in preliminary experiment, the rust distribution around steel cross section under different galvanic methods can be generated. The rust distributions of the four methods are relatively uniform, and the thickness difference of the rust layer is not too large (between 50 and 100 μm), which is consistent with previous studies (Malumbela *et al*. 2010). However the rust distributions under different methods are oriented in different direction. If one defines $\beta = \frac{D_L}{D_S}$ (D_L/D_S is the average rust layer thickness on larger/smaller side of the reinforcement) as the non-uniform coefficient of the corrosion. As such, the greater of β, the difference in thickness of the rust layer on both sides is greater, implying a higher level of non-uniformity. β of different methods are listed in Table 1. It is clearly seen that the tendency of non-uniform corrosion occur mainly in internal electrode methods, in which the rust layer on the one side (near the auxiliary electrode) are generally higher than that of other side(near the cover),and the β is quite larger than others. This finding supports that compared to other methods, the internal electrode method is the easiest to achieve non-uniform corrosion.

Table 1. β value of different methods

Method	B
External electrode methods(whole submerged in saline)	1.045
External electrode methods(part submerged in saline)	1.040
External electrode methods(sponge and stainless mesh)	1.107
Internal electrode method	1.354

4.0 NUMERICAL INVESTIGATION

4.1 FEM simulations

Further to investigate the electrochemical process under different acceleration methods, Finite element method (FEM) simulations were performed. This would assist to optimizing the selection of experimental parameters to reach targeted corrosion pattern of rebar in concrete. The commercial software Comsol Multiphysics® was used to establish the FEM simulations. As shown in Fig. 9. The geometrical model is comprised of a large square (t1) with dimensions of 100 mm × 100 mm representing the concrete, a circle (c1) with a diameter of 10 mm representing the rebar, and another circle (c2) with the same diameter representing the auxiliary electrode. For method (1) and (2), the square (t2) with dimensions of 150 mm × 200 mm represents saline in which the samples submerge. For method (3) a square shell (h1) with the thickness of 10 mm was established to representing the sponge and it is coated by a film (f1) which represents the stainless mesh. The minimum distance between the reinforcement and the auxiliary electrode is denoted by s, which is 75 mmx75 mmx30 mm and 40 mm from method (1) to (4). The concrete specimens were assumed to be completely saturated.

4.2 Numerical results

The plots of current density distribution around the reinforcement are shown in Fig. 10, in which the warmth of color represents the magnitude of corrosion current density and the arrows directs the movement of electric current. As is clearly indicated in the figure, the electric moves from the rebar to the stainless bar (mesh) and the current density has oriented in its distribution. The current density is highest at points close to the auxiliary electrode, while lowest at the opposite position. It is clear that this situation occurs obviously in internal electrode

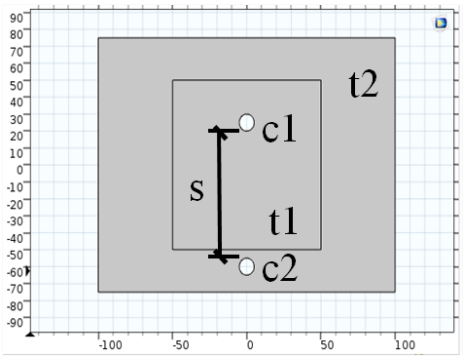

(a) External electrode methods, in which samples whole submerged in saline

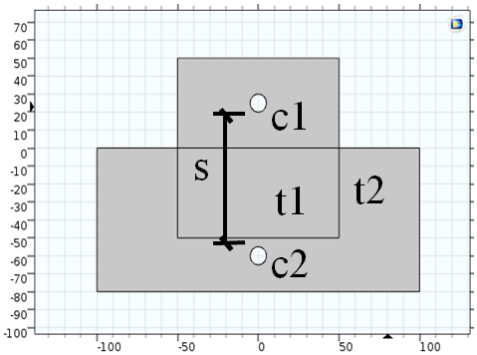

(b) External electrode methods, in which samples part submerged in saline

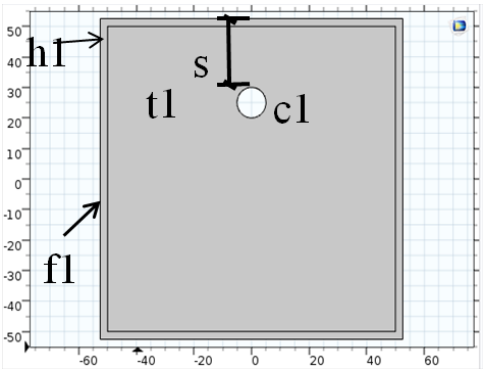

(3) External electrode method, samples wrapped by sponge and stainless mesh

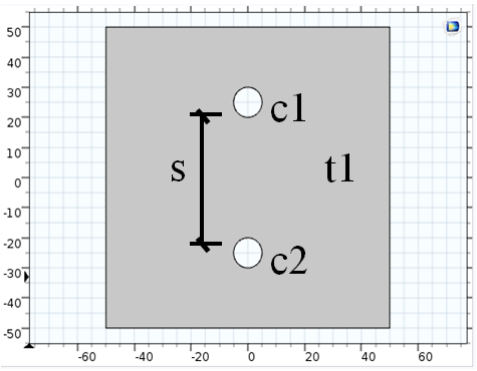

(4)Internal electrode methods

Fig. 9. Geometrical model for the FEM analysis

method, which is consistent with the experiment results.

In addition, according to previous derivation, distance between electrodes can influence the pattern of corrosion around rebar under the present electrochemical accelerated methods. As such, the following studies present the parameter analysis of this variable. γ=i_L/i_s(i_L/i_s is the average current density on larger/smaller side of the reinforcement) was defined as the non-uniform coefficient of the corrosion density. Figure 11(a) shows the evolution of γ as a function of change of s (move away from the reinforcement), at the interval of 5 mm. It can be seen that as the change of s increases, the γ of internal electrode method declines considerably while the γ of other methods relatively unchanged. Figure 11(b) indicates the influence of change of s on the distribution of current density, in which the intensity of streamlines represents the magnitude of current density. It is clear that the closer the electrodes are, the more intensive the streamlines between the electrodes will be. This imply that changing s can efficiently change the distribution of current density around reinforcement.

5.0 FURTHER VERIFICATION

Based on the numerical analysis and preliminary experiment, it has demonstrated that the pattern of corrosion proposed by internal electrode method is most similar to non-uniform corrosion in the present electrochemical accelerated methods. The orientation of anode and cathode and the distance between electrodes play an important role in the current density distribution in the specimens. According to this, the stainless wire was put into the cylinder samples parallel to the rebar as a cathode, as a modified internal electrode method which was given in following study.

In order to compare the FEM result with the experiment result, the further experiment carried out in four different circumstances as in Table 2. In the specimen ID, the A and B represent two different arrangement orientation of the auxiliary electrode relative to the rebar as shown in Fig. 12. Other parameters adopted the same meanings as those in previous sections.

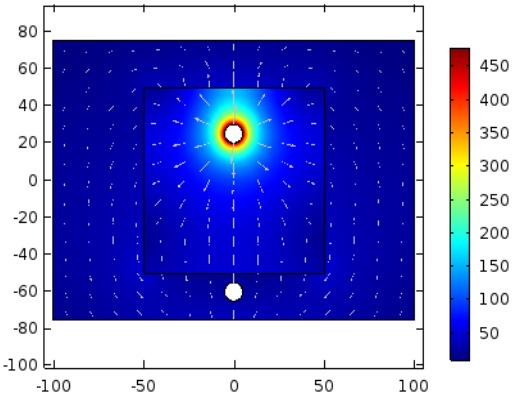

(a) External electrode methods, in which samples whole submerged in saline

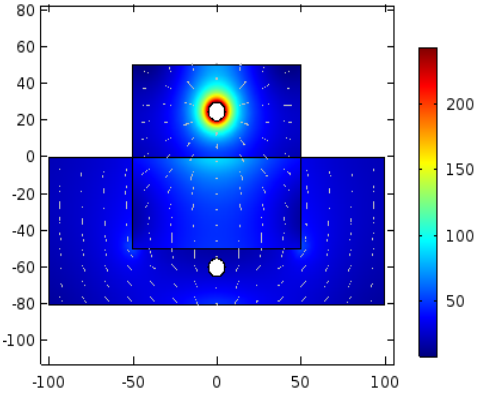

(b) External electrode methods, in which samples part submerged in saline

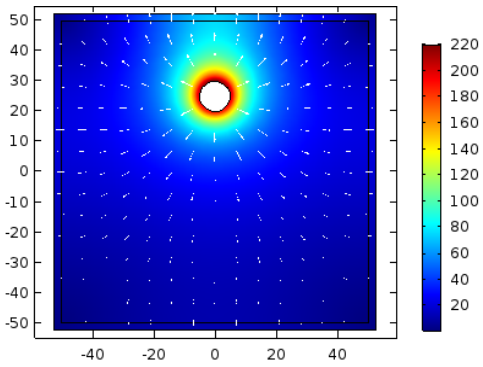

(c) External electrode methods, in which samples wrapped by sponge and stainless mesh

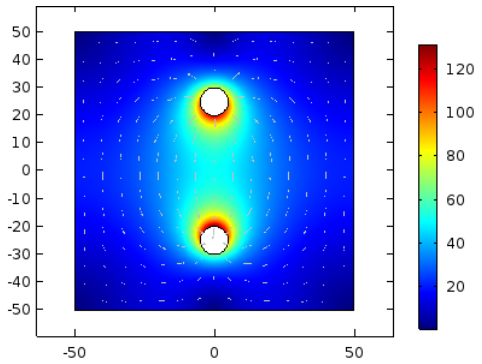

(d)Internal electrode methods

Fig.10. Current density distribution around the reinforcement (Unit: mm for geometry and A/m^2 for current density)

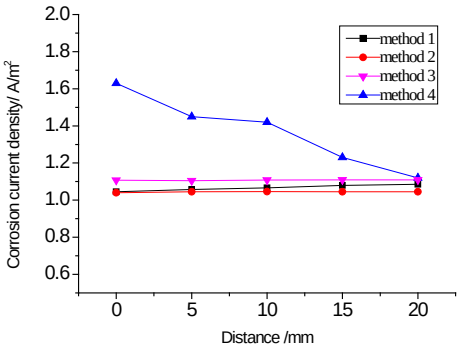

(a) Evolution of y as a function of change of s

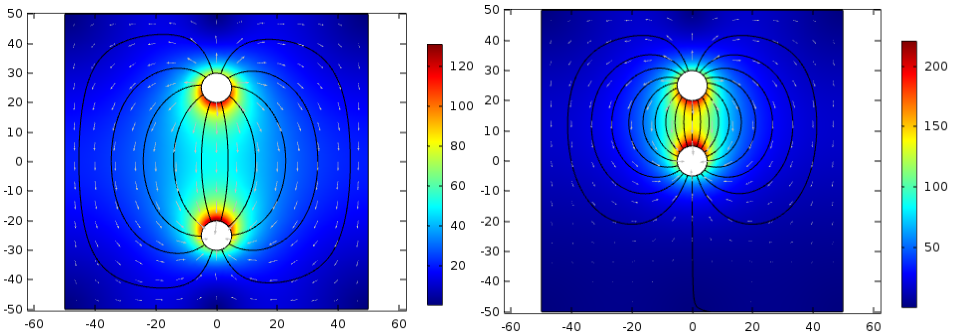

(b)The corrosion current density influenced by change of s under the internal electrode method

Fig.11. Influence of the change of distance between electrodes

Table 2. The geometrical parameters of the specimens

Specimen ID	Rebar Diameter (mm)	Distance between Electrodes (mm)
A12-6	12	6
B12-6	12	6
A12-2.5	12	2.5
A12.17	12	17

Note:The diameter of auxiliary electrode(stainless wire) was kept at 1.0 mm for all specimens

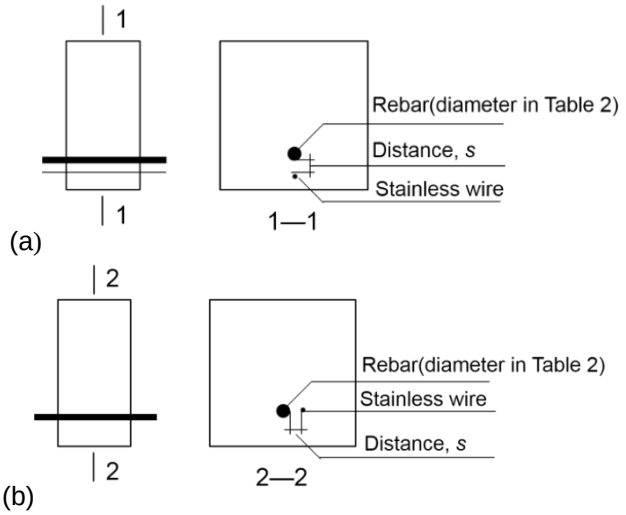

Fig. 12. Configuration of specimens(100 mm × 100 mm× 50 mm, with the cover thickness being 20 mm) with two different placement orientations of the auxiliary electrode(stainless wire) relative to the rebar. (a) Arrangement position A; (b) Arrangement position B.

The result of experiment shows that the rust only occur on the side where the auxiliary electrode locates, which imply that the position of electrode can decide the location of rust. The distribution of electrode can be considered as non-uniform corrosion. In addition, the maximum thickness of rust in A12-6 is 96.7 μm, the distribution range of rust is 127°, which is similar to B12-6 with the maximum thickness of 96.13 μm and the distribution range of 130°. Furthermore, Fig. 13 shows the evolution of rust distribution as the change of distance between electrodes. It clearly shows the effect of distance between electrodes. As the distance increase, the maximum thickness has decreased. It should be note that when the distance increase, the range of rust has also increased. Based on this, a position-controllable accelerated corrosion method can be established.

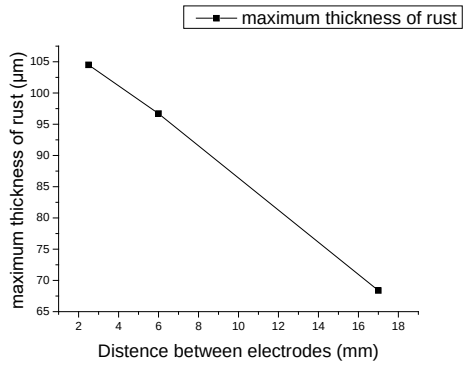

(a) Evolution of maximum thickness of rust as a function of change of s

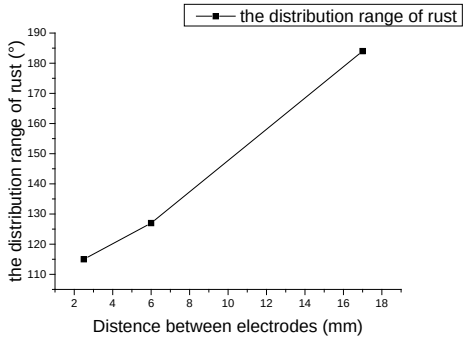

(b) Evolution of the range of of rust as a function of change of s

Fig.13. Evolution of distribution of rust under different distance of electrodes

6.0 CONCLUSIONS

This paper reported a preliminary study of electrochemical accelerated corrosion methods. The electrochemical mechanism of these four accelerated method were analyzed by using the FE software COMSOL. In terms of corrosion products distribution characteristic along the rebar circumference, the similarity of electrochemical accelerated and natural corrosion was presented. The results indicated that:

(1) Rebar corrosion with external electrode method can be regarded as uniform corrosion;

(2) The internal electrode method could result in a non-uniform corrosion, the orientation of anode and cathode and the distance between electrodes and distance between rebar and auxiliary electrode are two major influence parameters for accelerated non-uniform corrosion;

(3) Based on the corrosion electrochemical principles, a modified internal electrode method was given. This method can be used to simulate the natural corrosion of rebar with the same corrosion product distribution.

Acknowledgement

The financial support from the National Basic Research Program (973 Program) (Grant No.2015CB655103) of the People's Republic of China and the National Natural Science Foundation (Grant Nos.51678529 and 51578497) is gratefully acknowledged.

References

B.H. Oh, K.H. Kim, B.S. Jang, Critical corrosion amount to cause cracking of reinforced concrete structures, ACI materials journal, 106 (2009) 333-339.

C. Fu, N. Jin, H. Ye, X. Jin, W. Dai, Corrosion characteristics of a 4-year naturally corroded reinforced concrete beam with load-induced transverse cracks, Corrosion Science, 117 (2017)504 11-23.

C. Cao, M.M. Cheung, Non-uniform rust expansion for chloride-induced pitting corrosion in RC structures, Construction and Building Materials, 51 (2014) 75-81.

G. Malumbela, M. Alexander, P. Moyo, Interaction between corrosion crack width and steel loss in RC beams corroded under load, Cement and Concrete research, 40 (2010) 1419-1428.

H. Ye, Y. Tian, N. Jin, X. Jin, C. Fu, Influence of cracking on chloride diffusivity and moisture influential depth in concrete subjected to simulated environmental conditions, Construction and Building Materials, 47 (2013) 66-79.

R.W. Revie, Corrosion and corrosion control, John Wiley & Sons2008.

R. Mann, J. Amphlett, B. Peppley, C. Thurgood, Application of Butler–Volmer equations in the modeling of activation polarization for PEM fuel cells, Journal of power sources, 161 (2006)582 775-781.

T.A. El Maaddawy, K.A. Soudki, Effectiveness of impressed current technique to simulate corrosion of steel reinforcement in concrete, Journal of materials in civil engineering, 15 (2003)567 41-47.

X. Zhang, J. Wang, Y. Zhao, L. Tang, F. Xing, Time-dependent probability assessment for chloride induced corrosion of RC structures using the third-moment method, Construction and Building Materials, 76 (2015) 232-244.

Y. Yuan, Y. Ji, S.P. Shah, Comparison of two accelerated corrosion techniques for concrete structures, ACI Structural Journal, 104 (2007) 344.

Y.Yuan, X. Zhang, Y. Ji . A comparative study on structural behavior of deteriorated reinforced concrete beam under two different environments [J] .China Civil Engineering Journal 2006, 39 (3): 42-46. (in Chinese)